

Driving Style Analysis Using Primitive Driving Patterns With Bayesian Nonparametric Approaches

Wenshuo Wang^{ID}, Student Member, IEEE, Junqiang Xi^{ID}, and Ding Zhao^{ID}

Abstract—Driving style analysis plays a pivotal role in intelligent vehicle design. This paper presents a novel framework for driving style analysis based on primitive driving patterns. To this end, a Bayesian nonparametric approach based on a hidden semi-Markov model (HSMM) is introduced to extract the primitive driving patterns from multi-dimensional time-series driving data without prior knowledge of these driving patterns. For the Bayesian nonparametric approach, a hierarchical Dirichlet process (HDP) is applied to learn the unknown smooth dynamical modes in the HSMM, called primitive driving patterns. Two other types of Bayesian nonparametric approaches (HDP-HMM and sticky HDP-HMM) are developed as comparatives in order to show the advantages of the HDP-HSMM. The naturalistic car-following data of 18 drivers are collected from the University of Michigan Safety Pilot Model Deployment database. For each driver, 75 primitive driving patterns are semantically predefined according to their physical and psychological perception thresholds. The individual driving styles are then semantically analyzed based on the distribution over primitive driving patterns, and the similarity of driving styles among drivers is then evaluated. Experimental results demonstrate that the utilization of driving primitive pattern provides a semantically interpretable way to analyze driver’s behavior and driving style.

Index Terms—Driving style, hidden Markov model, car-following behavior, Bayesian nonparametric approach, behavioral semantics.

I. INTRODUCTION

DIVING style has a great impact on eco-driving [1], road safety [2], and intelligent vehicles [3], [4]. *Driving style*, in this paper, refers to a set of dynamic activities/steps that a driver uses when driving, according to his/her personal judgment, experience and skills [2], [5], [6]. Previous research focused on characterizing and analyzing driving style by directly utilizing the statistical metrics of measured driving data. For example, the mean, standard deviation, and maximum of brake pressure, throttle position and acceleration were

Manuscript received August 14, 2017; revised January 1, 2018, June 9, 2018, and September 10, 2018; accepted September 12, 2018. Date of publication October 24, 2018; date of current version July 31, 2019. This work was supported by the China Scholarship Council (CSC). The Associate Editor for this paper was Y. Gao. (*Corresponding authors:* Junqiang Xi; Ding Zhao.)

W. Wang is with the Department of Mechanical Engineering, Beijing Institute of Technology, Beijing 100081, China, and also with the Department of Mechanical Engineering, University of California at Berkeley, Berkeley, CA 94720 USA (e-mail: wwsbit@gmail.com).

J. Xi is with the Department of Mechanical Engineering, Beijing Institute of Technology, Beijing 100081, China (e-mail: xijunqiang@bit.edu.cn).

D. Zhao is with the Department of Mechanical Engineering, University of Michigan, Ann Arbor, MI 48109 USA (e-mail: zhaoding@umich.edu).

Digital Object Identifier 10.1109/TITS.2018.2870525

used to classify drivers [7], [8] towards safety-driving and eco-driving [9], [10]. The F-score with mean and standard deviation was also used to take multidimensional driving style inventory [11]. Based on these indicators, researchers usually apply machine learning techniques to driving style recognition with a well-trained classifier such as support vector machine (SVM) [12], [13], semi-supervised support vector machine (S³VM) [14] and neural networks [8]. With the statistical indicators, these above-mentioned approaches are able to capture the static driving characteristics, but they are limited to describe the dynamic process of drivers’ behavioral semantics.

Decomposing complex driver behavior into simple, smaller and primitive patterns can facilitate driving style analysis and identification [15]. *Primitive driving pattern*, as generally defined in this paper, is the primitive segments that can be viewed as the basic building blocks of driver behavior. For example, drivers’ car-following behavior can be roughly decomposed into three primitive driving patterns: closing in, keeping, and falling behind. Segmenting long-term time-series driver behavior data into smaller components allows to gain insight into the driver’s dynamic decision-making process [16], [17] and driving style [15]. Driving pattern definition is related to how driving patterns are characterized, allowing a human or algorithmic observer to identify driving patterns from measured data. These definitions are often subjective, application-driven, algorithmic-dependent, and tend to group into three categories:

1) *Physical Boundaries*: The definition of a pattern typically refers to a physical change that occurs when a driver’s distinguishable operation/decision starts or ends. These natural physical boundaries could be specified by changes of vehicle steering angle, brake/accelerator pedal position or their combination [18]. These domain knowledge characteristics may be specific to a particular operation (e.g., turn left or turn right) or could generalize multiple operations (e.g., acceleration and lane change). For example, MacAdam, *et al.* [19] manually classified car-following behavior into five patterns (i.e., closing in rapidly, close in, following, falling behind, and falling behind rapidly) based on the predefined thresholds of relative speed and relative distance, and then trained a neural network classifier to evaluate the drivers’ driving style. The lane-change behavior can also be segmented into different patterns depending on vehicle position in the lane and the position with respect to surrounding vehicles [20]–[22]. In general, the physical

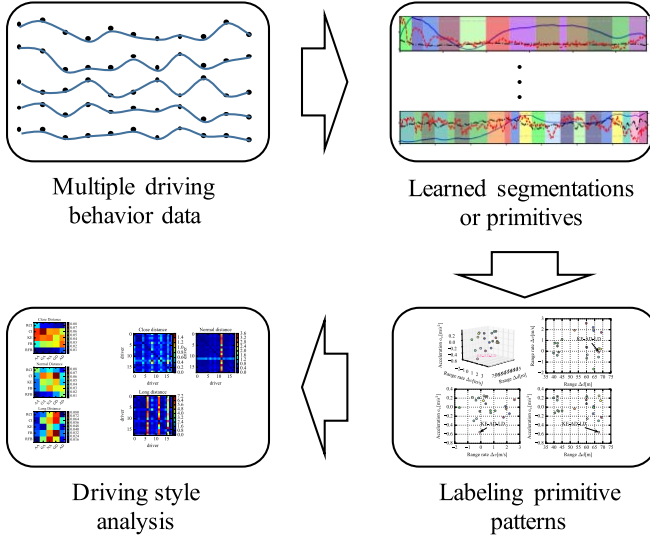


Fig. 1. The proposed driving primitive-based framework capable of semantically analyzing driving styles.

boundaries are empirically set according to suit requirements, which are more subjective.

2) *Template Boundaries*: Driving pattern can be defined by a user-provided template. One of the most popular template-based algorithms is the dynamic time warping, which has been applied to car-following behavior analysis [23]. Defining primitive patterns by a template or a template set allows maximizing flexibility for users depending on special requirements. However, this approach is usually time-consuming for preparing the templates and may miss some special and meaningful templates.

3) *Derived Metrics Boundaries*: A primitive driving pattern can also be defined by a change in derived metrics (e.g., variance) or derived signals (e.g., hidden Markov model state transitions) based on supervised and unsupervised approaches. For example, Ma and Andreasson [24] directly implemented a consolidated fuzzy clustering algorithm to classify different car-following regimes and obtained five car-following patterns. Higgs and Abbas [15] developed a two-step clustering algorithm to segment drivers' car-following behavior based on eight predefined state-action variables (longitudinal acceleration, lateral acceleration, yaw rate, vehicle speed, lane offset, yaw angle, range, and range rate). This method resulted in 30 state-action clusters corresponding to driving patterns. These aforementioned approaches, however, require prior knowledge about patterns or clusters. Moreover, they subjectively define and extract these driving patterns with excessive effort and may lead to bias due to the diversity of prior knowledge of different data analysts.

Differing from previous research that selects the statistical features (e.g., mean and standard deviation) of the measured driving data and that manually defines patterns to characterize driving styles, in this paper, we proposed a framework for driving style analysis based on driving primitive patterns (Fig. 1). The primitive driving pattern can reflect drivers' driving preferences and the dynamic process

of behavioral semantics. In our approach, rather than subjectively relying on hand-tuned models or predefined rules to select primitive driving patterns like in [15], [19], and [24], we implement the Bayesian nonparametric approaches to directly learn primitive driving patterns from time-series data without requiring prior knowledge about these patterns. For this purpose, a hierarchical modeling structure is developed by combining a hierarchical Dirichlet process (HDP) with a hidden semi-Markov model (HSMM). The primitive driving patterns are then semantically labeled for each driver according to their physical and psychological perception thresholds using K-means clustering. Finally, the distribution of primitive driving patterns is used to analyze individual driving styles and to illustrate the similarity between drivers with an entropy index (i.e., Kullback-Leibler divergence). This work presents the following contributions:

- 1) Introducing a novel framework for driving style analysis based on primitive driving patterns.
- 2) Implementing Bayesian nonparametric approaches to automatically extract interpretable driving primitive patterns.
- 3) Analyzing behavioral semantics and driving styles of the extracted driving primitives based on K-means clustering algorithms for car-following behaviors.

The remainder of this paper is organized as follows. Section II introduces the Bayesian nonparametric approach based on a hidden Markov model (HMM) and its extensions. Section III presents driving data collection and preprocessing. Section IV shows the experimental results of primitive driving patterns using different approaches. Section V analyzes the results of driving styles. Lastly, the conclusion is made in Section VI.

II. BAYESIAN NONPARAMETRIC LEARNING APPROACHES

Bayesian nonparametric learning has shown its powerful ability to model and predict driver behaviors [25]–[27] with the priorly unknown driving patterns. In this section, we will introduce the Bayesian nonparametric approaches. In order to capture this idea easily, we first present some basic concepts, including HMM, HSMM, HDP, HDP-HMM, and sticky HDP-HMM.

A. HMM-Based Approaches

1) *Hidden Markov Model*: In this work, the dynamic driving behavior is treated as a Markov process, and thus, it can be modeled based on the structure of HMM. The core of HMM consists of two layers: a layer of hidden *state* and a layer of *observation* or *emission*, as shown in Fig. 2(a), where the shaded nodes are observations, y_t , and the unshaded nodes are latent states x_t , i.e., primitive driving patterns in this paper. The hidden state sequence, $\mathbf{x} = \{x_t\}_{t=1}^T$, is a sequence of primitive driving patterns over a finite set \mathcal{X} with $x_t \in \mathcal{X}$. The transition probability from primitive driving patterns i to j is noted as $\pi_{i,j} = p(x_{t+1} = j | x_t = i)$ and the transition matrix between these patterns is $\boldsymbol{\pi} = \{\pi_{i,j}\}_{i,j=1}^{|\mathcal{X}|}$, where $|\mathcal{X}|$ indicates the size of pattern set \mathcal{X} . The distribution of observations

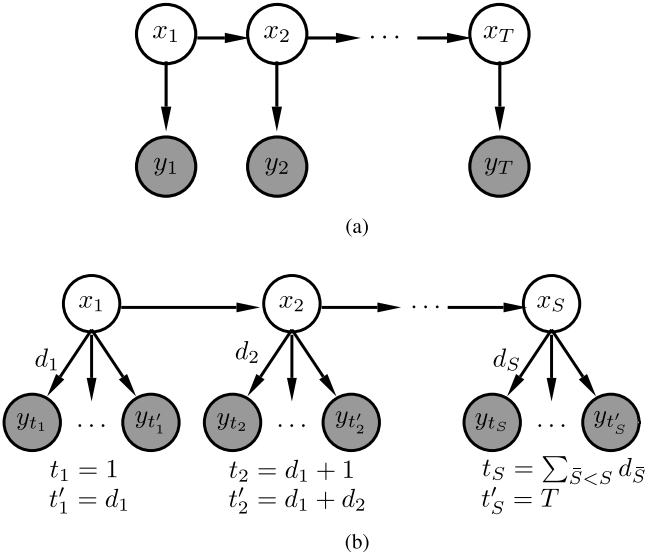


Fig. 2. A graphical model of HMM and HSMM. Shaded nodes are the observable states and unshaded nodes are the latent modes. (a) Hidden Markov model. (b) Hidden semi-Markov model.

or emissions y_t given current hidden states is defined by $p(y_t|x_t, \theta_i)$, where θ_i is the emission parameter for mode i . Thus, we can describe HMM by

$$x_t|x_{t-1} \sim \pi_{x_{t-1}} \quad (1a)$$

$$y_t|x_t \sim F(\theta_{x_t}) \quad (1b)$$

where $F(\cdot)$ is an indexed family of distribution.

2) *Hidden Semi-Markov Model*: The hidden semi-Markov model (HSMM), as an extension of HMM, is traditionally defined by allowing the underlying process to be a semi-Markov chain, which means that each state has a variable duration [28], as shown in Fig. 2(b). Several approaches can be used to define HSMM depending on the assumptions and applications. In this paper, we assume that each hidden state's duration is given over an explicit distribution, called explicit duration HMM [29]. Therefore, we augment the generative process of a standard HMM with a random state duration time, drawn from some state-specific distribution when the state is entered [30]. Here, we use the random variable d_t to denote the duration of a state that enters at time t , and $p(d_t|x_t = i)$ denotes the probability mass function for d_t . Similar to HMM, we define HSMM by

$$x_s|x_{s-1} \sim \pi_{x_{s-1}} \quad (2a)$$

$$d_s \sim g(\omega_s) \quad (2b)$$

$$y_t|x_s, d_s \sim F(\theta_{x_s}, d_s) \quad (2c)$$

where $g(\omega_s)$ is a state-specific distribution over state duration d_s and ω_s is the parameter prior of duration distributions.

3) *Hierarchical Dirichlet Process*: As aforementioned in Section I, the number of latent dynamic modes in (1) and (2) is priorly unknown, and the modes of HMM and HSMM are subject to a specific distribution defined over a measure space.

The *Dirichlet process* (DP) is a measure on measures [31], denoted by $DP(\gamma, H)$, and provides a distribution over discrete

probability measures with an infinite collection of atoms [32]

$$G_0 = \sum_{i=1}^{\infty} \beta_i \delta_{\theta_i}, \quad \theta_i \sim H \quad (3a)$$

$$\beta_i = v_i \prod_{\ell=1}^{i-1} (1 - v_\ell), \quad v_i \sim \text{Beta}(1, \gamma) \quad (3b)$$

on a parameter space Θ that is endowed with a base measure H . Here, β_i are the weights sampled by a stick-breaking construction [31] and we denote $\beta \sim \text{GEM}(\gamma)$, with $\beta = [\beta_1, \beta_2, \dots]$.

According to the above discussion, an HDP [31] is able to be used to define a prior on the set of HMM transition probability measures G_j

$$G_j = \sum_{i=1}^I \pi_{ji} \delta_{\theta_i} \quad (4)$$

where δ_θ is a mass concentrated at θ . Assuming that each discrete measure G_j is a variation on a global discrete measure G_0 , thus the Bayesian hierarchical specification takes $G_j \sim \text{DP}(\alpha, G_0)$, where G_0 draws from a $\text{DP}(\gamma, H)$, i.e.,

$$G_0 = \sum_{i=1}^{\infty} \beta_i \delta_{\theta_i}, \quad \beta|\gamma \sim \text{GEM}(\gamma) \quad (5a)$$

$$G_j = \sum_{i=1}^{\infty} \pi_{ji} \delta_{\theta_i}, \quad \pi_j|\alpha, \beta \sim \text{DP}(\alpha, \beta) \quad (5b)$$

$$\theta_i|H \sim H \quad (5c)$$

where $\pi_j = [\pi_{j1}, \pi_{j2}, \dots]$.

4) *Sticky HDP-HMM & HDP-HSMM*: Based on the above discussion, by applying the HDP prior to HMM and HSMM, we can obtain HDP-HMM and HDP-HSMM [30], respectively, as shown in Fig. 3.

For the sticky HDP-HMM(γ, α, H) [31], by adding an extra parameter $\kappa > 0$ that biases the process toward self-transition in (5b), increasing the expected probability of self-transition by an amount proportional to κ [32], we can obtain

$$\beta|\gamma \sim \text{GEM}(\gamma) \quad (6a)$$

$$\pi_i|\alpha, \beta, \kappa \sim \text{DP}(\alpha + \kappa, \frac{\alpha\beta + \kappa\delta_i}{\alpha + \kappa}), \quad i = 1, 2, \dots \quad (6b)$$

$$x_t|x_{t-1} \sim \pi_{x_{t-1}}, \quad t = 1, 2, \dots, T \quad (6c)$$

$$y_t|x_t, \theta_{x_t} \sim F(\theta_{x_t}), \quad t = 1, 2, \dots, T \quad (6d)$$

$$\theta_i|H \sim H, \quad i = 1, 2, \dots \quad (6e)$$

where T is the data length. Note that a larger value of κ will cause a greater self-transition probability and the original HDP-HMM is obtained when $\kappa = 0$ in (6b). Similarly, for HDP-HSMM(γ, α, H, G), we can describe it using [30]

$$\beta|\gamma \sim \text{GEM}(\gamma) \quad (7a)$$

$$\pi_i|\alpha, \beta \sim \text{DP}(\alpha, \beta), \quad i = 1, 2, \dots \quad (7b)$$

$$(\theta_i, \omega_i) \sim H \times G, \quad i = 1, 2, \dots \quad (7c)$$

$$z_s \sim \bar{\pi}_{z_{s-1}}, \quad s = 1, 2, \dots \quad (7d)$$

$$d_s \sim g(\omega_{z_s}), \quad s = 1, 2, \dots \quad (7e)$$

$$x_{t_s^1:t_s^{d_s+1}} = z_s \quad (7f)$$

$$y_{t_s^1:t_s^{d_s+1}} = F(\theta_{x_t}) \quad (7g)$$

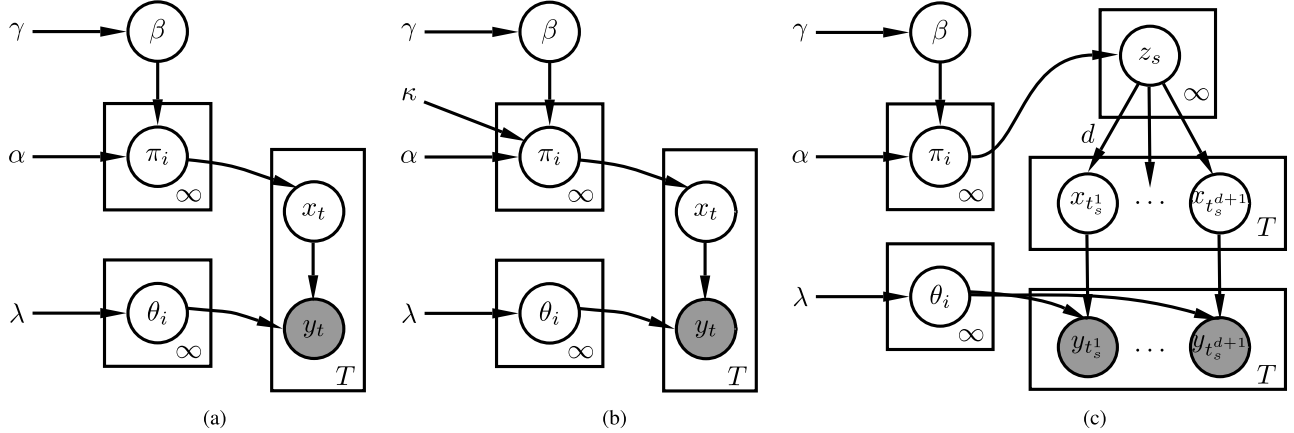


Fig. 3. Graphical models of three Bayesian nonparametric HMM-based approaches for an univariate time series data with a length T . (a) HDP-HMM. (b) sticky HDP-HMM. (c) HDP-HSMM.

TABLE I
PARAMETER VALUES FOR MODELS

parameter	description	value
(a_α, b_α)	α gamma prior	(1,1)
(a_γ, b_γ)	γ gamma prior	(1,1)
(a_κ, b_κ)	κ gamma prior	(100,1)
n_0	IW prior degree of freedom	$N + 2$
S_0	IW prior scale	$0.75 \cdot \bar{\Sigma}$

where $\bar{\pi} = \frac{\pi_{ij}}{1-\pi_{ii}}(1-\delta_{ij})$ is used to estimate self-transition in the state sequence z_s .

B. Observation (or Emission) Model

The observation model is determined by the type of function $F(\theta_i)$, which can be Gaussian emissions [33] or switch linear dynamic models (SLDSs) [32] (e.g., vector autoregressive). One main challenge with non-parametric approaches is that one must derive all the necessary expressions to properly perform inference [34]. In order to make our algorithm computationally tractable, we assume that observations are drawn from a Gaussian distribution [33]. When observations are assumed to be drawn from a Gaussian distribution, the θ_i can be set as $\theta_i = [\mu_i, \Sigma_i]$. Therefore, if the priors for observations and transition distributions are learned correctly, the full-conditional posteriors can be computed using Gibbs sampling method. Johnson and Willsky [30] present further details of the inference method using Gibbs sampling methods.

C. Learning Procedure

We develop and test these aforementioned models based on Johnson and Willsky's pyhsmm¹ module [30] and Fox's code² [35]. And the hyperparameters are determined using following rules:

- 1) We place a Gamma(a, b) prior on the hyperparameters γ, α , and κ [25], [32], as shown in Table I, where N is the dimension of input data.
- 2) The Inverse-Wishart (IW) prior is conjugate to the Gaussian distributions [36] and SLDS parameter set [32], thus the hyperparameters for θ_i are taken

to be from an IW with a hyper-parameter γ , that is,

$$\Sigma_i | n_0, S_0 \sim \text{IW}(n_0, S_0) \quad (8)$$

where n_0 is IW prior degree of freedom, S_0 is the IW prior scale, and $S_0 = 0.75 \bar{\Sigma}$, where $\bar{\Sigma}$ is the covariance of the observed data.

In addition, the observation variables are generated from a Gaussian model and we set $\mu_i = 0$ according to [25].

III. CAR-FOLLOWING DATA COLLECTION AND PREPROCESSING

This section will show the application of the developed methods to driving style analysis regarding car-following behavior. The data collection and processing procedures are presented as follows.

A. Equipment and Participants

All driving data we used were extracted from the Safety Pilot Model Deployment (SPMD) database, which recorded the naturalistic driving of 2,842 equipment vehicles in Ann Arbor, Michigan, for more than two years. We selected 18 equipped passenger cars (i.e., 18 drivers) to collect on-road data. The experiment vehicles were equipped with data acquisition systems and Mobileye (Fig. 4). The road information (e.g., lane width and lane curvature) and the surrounding vehicle's information (e.g., relative distance and relative speed) were recorded by Mobileye. The subject vehicle information such as speed, steering angle, and acceleration/brake pedal position were extracted from CAN-bus signal at 10 Hz.

Drivers had an opportunity to become accustomed to the equipped vehicles. They performed casual daily trips for several months without any restrictions on or requirements for their trips, the duration of the trips, or their driving style. The data processing and recording equipment were hidden from the drivers, thus avoiding the influence of recorded data on driver behavior.

B. Data Extraction and Preprocessing

In order to extract the car-following behavior data capable of characterizing drivers' dynamic preference (Fig. 5), we selected the following variables according to [37]–[39]:

- 1) The subject vehicle acceleration a_x , which can directly reflect driver intent and driving preference.

¹<https://github.com/mattjj/pyhsmm>

²<https://www.stat.washington.edu/~ebfox/software.html>



Fig. 4. Example of equipment for data collection. (a) Vehicle; (b) Mobileye; and (c) Data acquisition systems.

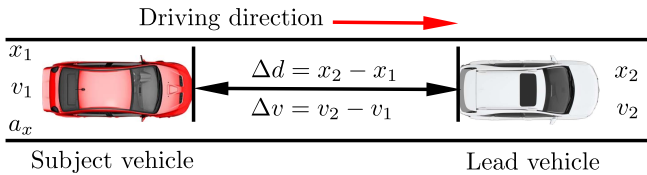


Fig. 5. Car-following scenarios.

- 2) The relative range (Δd) between the subject vehicle and the lead vehicle, computed by $\Delta d = x_2 - x_1$. It can reflect driver's preference in headway, where x_1 and x_2 are the global positions of the subject vehicle and the lead vehicle, respectively.
- 3) The relative range rate ($\Delta v = v_2 - v_1$). It can capture the dynamical relationship between two vehicles, where v_1 and v_2 are the speeds of the subject vehicle and the lead vehicle, respectively.

Hence the car-following data consisting of the three feature variables were extracted from the SPMD database under the following conditions: (1) There was a lead vehicle at the same lane with the subject vehicle; (2) the lead distance was less than 120 m; (3) the vehicle speed was greater than 18 km/h (i.e., 5 m/s); (4) if a surrounding vehicle was cutting in, then the car-following event ended; (5) the duration of each single car-following event was greater than 50 s [40]. Fig. 6 displays the trajectories of all car-following events in the SPMD database.

In order to reduce the scale influence of different variables on the segmentation results, we additionally normalized each variable of observation vector for each event before training a model so that the empirical variance of the set was equal to one by

$$\bar{y}_m^{(l)} = \frac{\mathbf{y}_m^{(l)} - \boldsymbol{\mu}_m}{\sigma_m}, \quad l = 1, 2, \dots, L, \quad m = 1, 2, \dots, M \quad (9)$$

where $\mathbf{y} = [\Delta d, \Delta v, a_x]^T$, l is the number of event, $\boldsymbol{\mu}_m$ and σ_m are the mean and covariance of all events for m^{th} driver, with $M = 18$. Then we applied the Bayesian nonparametric learning approaches presented in Section II to segment the normalized time-series data.

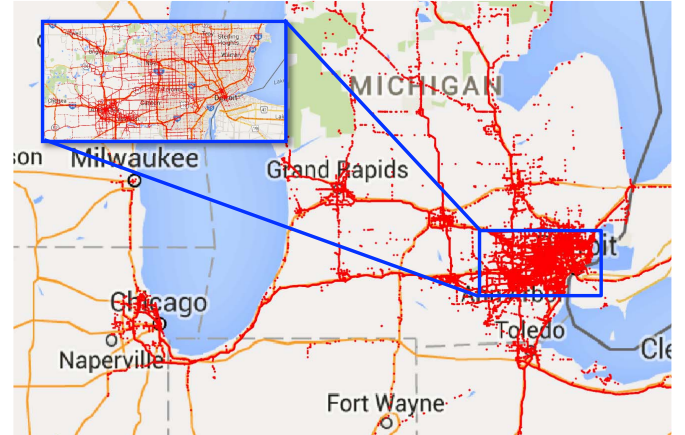


Fig. 6. Path of all car-following events.

TABLE II
VARIABLE SEGMENTATION

Variable	Variable state	Threshold
Range [m]	Long distance (LD)	> 57.33
	Normal distance (ND)	[27.32, 57.33]
	Close distance (CD)	[5.00, 27.32]
Range rate [m/s]	Rapidly closing in (RCI)	< -0.90
	Closing in (CI)	[-1.17, -0.21]
	Keeping (KE)	[-0.21, 0.33]
	Falling behind (FB)	[0.33, 1.29]
Acceleration [m/s ²]	Rapidly falling behind (RFB)	> 1.29
	Aggressive acceleration (AA)	> 0.23
	Gentle acceleration (GA)	[0.06, 0.23]
	No acceleration (NA)	[-0.07, 0.06]
	Gentle deceleration (GD)	[-0.24, -0.07]
	Aggressive deceleration (AD)	< -0.24

C. Variable Segmentation and Threshold Selection

In order to easily make a semantic interpretation for primitive driving patterns, we classify each variable into different levels based on drivers' physical and psychological perception thresholds corresponding to their statistical feature, as shown in Table II. More specifically, we fit them using different distributions to determine the thresholds for each variable from the statistical perspective.

Fig. 7(a) shows the fitting results of the relative range (Δd), relative range rate (Δv), and subject vehicle acceleration (a_x) using four distributions, including normal distribution (\mathcal{N}), Beta distribution (\mathcal{B}), Student- t distribution (t), and Gamma distribution (Γ) [41]. It can be seen that: 1) for range rate and acceleration, the t -distribution achieves a better fitting performance than other three distributions, and 2) for the range, the Γ -distribution and the \mathcal{B} -distribution obtain a better fitting performance than other two distributions. According to the perceptible characteristics of variables and human driver's comfortable/perception thresholds, we select the percentile value of range based on the Γ -fitting results, and select the percentile values of range rate and acceleration based on the t -fitting results (Fig. 7(b)). This procedure is discussed as follows:

- Relative range (Δd): Relative range is classified into three levels: long distance (LD), normal distance (ND), and close distance (CD). Note that from the top plot of Fig. 7(a), the lower threshold of 27.32 m matches

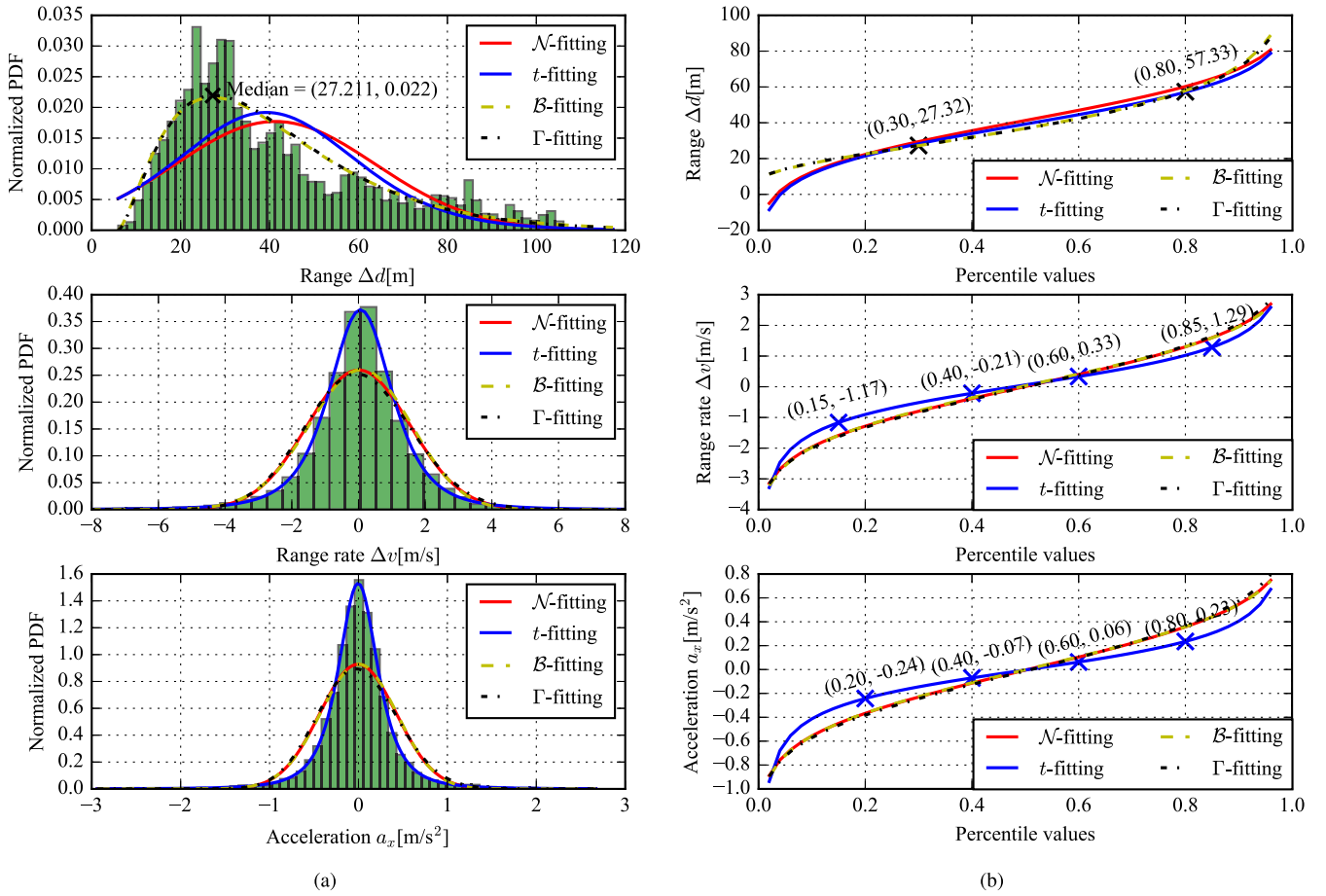


Fig. 7. (a) The statistical fitting results and (b) threshold values of three variables using four distributions, i.e., Normal (\mathcal{N}) distribution, Beta (\mathcal{B}) distribution, Student- t (t) distribution, and Gamma (Γ) distribution.

the median value 27.21 m and the upper threshold of 57.33 m is close to the threshold 61 m which is usually used to distinguish the free-flow regime [42]. Therefore, the threshold 30 and 85 percentile values of headway distance are selected.

- Relative range rate (Δv): Existing research demonstrates that drivers' velocity difference perception threshold is $|\Delta v^{\text{thr}}| \in [0.05, 0.2]$ m/s [43]. Hence it is conservative enough to assume that human driver hardly feels the change of range rate when $|\Delta v| < 0.2$ m/s. In addition, human driver can distinctly feel the change of range rate when $|\Delta v| > 1.3$ m/s [44]. Therefore, the thresholds are selected the percentile values of 15, 40, 60, and 85 for range rate, corresponding to the range rate of -1.17 m/s, -0.21 m/s, 0.33 m/s, and 1.29 m/s, respectively, as shown in Table II and the middle plot of Fig. 7(b). Thus, the range rate is divided into five segments [19]: rapidly closing in (RCI), closing in (CI), keeping (KE), falling behind (FB), and rapidly falling behind (RFB).
- Acceleration (a_x): Acceleration is divided into five levels based on drivers' vestibular and kinesthetic thresholds $|a_x^{\text{thr}}| \approx 0.05$ m/s 2 [45] and longitudinal acceleration comfort threshold $|a_x^{\text{thr}}| \approx 0.2$ m/s 2 [46]. In this work, we use the percentile values of 20, 40, 60, and 80 for acceleration as the thresholds, with -0.24 m/s 2 , -0.07 m/s 2 , 0.06 m/s 2 , and 0.23 m/s 2 , which quantitatively match

the kinesthetic perception and comfort thresholds. Thus, the acceleration is segmented into aggressive acceleration (AA), gentle acceleration (GA), no acceleration (NA), gentle deceleration (GD), and aggressive deceleration (AD), as shown in Fig. 7(b) and Table II.

Based on the predefined thresholds of each variable, we finally obtain a primitive car-following pattern library with a size of 75 ($3 \times 5 \times 5 = 75$) by permuting the level of each feature variable in Table II. This makes it easy to semantically label the primitive pattern of time-series driving data, and provides a different perspective for driving style analysis.

IV. MODEL EVALUATION AND RESULT ANALYSIS

In this section, the method effectiveness for car-following behavior analysis and the learning results of primitive driving patterns are discussed.

A. Method Performance Evaluation

1) *Evaluation Method:* One standard approach to evaluate the model performance is using the leave-one-out cross-validation (LOO-CV) method with splitting data into training set and test set. However, the ground truth of the segmentation results for test dataset is difficult to obtain because of the unknown number and type of primitive driving patterns. Therefore, it is experimentally intractable to evaluate the model performance through comparing the learning results

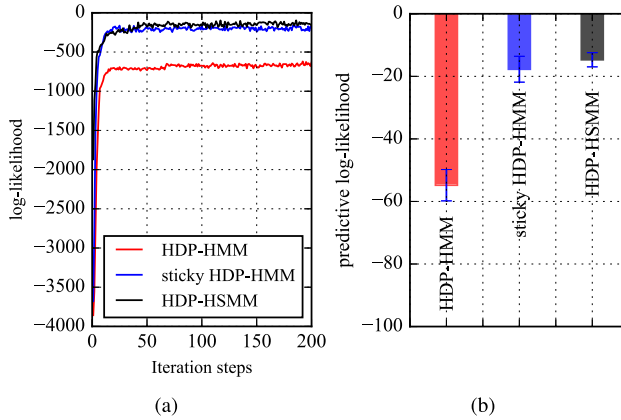


Fig. 8. (a) The log-likelihood of modeling the training data; (b) the predictive log-likelihood of test data for all three methods.

with the ground truth. We evaluate the effectiveness of the developed approaches based on the ability of the learned models to predict the duration of each primitive driving pattern for the test data. The predictive log-likelihood is employed to evaluate the fidelity of the learned models [27]. For each driver and corresponding test datasets, we use the training data to learn parameters of all three models, and the learned models are then used to predict the probability distribution of durations for each primitive driving pattern at each frame of the test data. The probability distribution of durations of primitive driving patterns is used to compute the predictive log-likelihood [27]. For each driver, the driving data are randomly and evenly grouped into ten folds. Nine folds are used for model training and the remaining one fold is used for model test. Thus we can finally obtain ten cross-validation results for each driver. During the training and testing procedures, the normalized car-following on-road data, \bar{y} , are used to learn the three model parameters and test these models.

2) *Results:* Fig. 8 shows the log-likelihood of modeling the training data and the predictive log-likelihoods of the test data with the LOO-CV procedure, given the training data for all methods. Experiment results show that HDP-HSMM obtains the highest log-likelihood of fitting training data (Fig. 8(a)) and the highest predictive log-likelihood on test data (Fig. 8(b)), indicating that HDP-HSMM outperforms HDP-HMM for segmenting drivers' car-following data sequences. Note that HDP-HSMM obtains a slightly higher log-likelihood value and lower standard deviation, compared to sticky HDP-HMM.

Simulations were performed on an Intel Core i7 laptop with a processor of 2.5 GHz. For one-hour driving data (i.e., 3.6×10^4 data samples), the HDP-HMM, sticky HDP-HMM, and HDP-HSMM took about 4.14 minutes, 5.37 minutes, and 7.72 minutes on average to learn model parameters, respectively. The results demonstrate that the nonparametric approaches are satisfactorily cost-effective.

B. Segmentation Results and Comparisons

For clarity and conciseness, we will show the results from representative trials of driver #0. An example of segmentation results with the three approaches is shown in Fig. 9. From Fig. 9(a), it can be noticed that HDP-HMM could not segment the driving patterns as expected. For example, the driving

data ranging from 0 s to 20 s obviously include the positive and negative values of range rate and acceleration – namely, the driver #0 presents the patterns of closing in and falling behind – but HDP-HMM does treat these behaviors as a single primitive pattern.

The sticky HDP-HMM (Fig. 9(b)) successfully segment time-series driving data, but it is sensitive to data fluctuation. For example, patterns with very short duration occur frequently (e.g., a pattern only lasts about 0.2 s), which is unexpected for describing drivers' driving states. The sticky HDP-HMM results in many patterns with duration less than 1.0 s, for example, durations are 0.2 s, 0.8 s, 0.1 s, 0.7 s, 0.3 s, 0.6 s at time 8.6 s, 32.2 s, 55.9 s, 58.8 s, 64.3 s and 64.7 s, respectively. In real driving cases, human driver obviously does not frequently adjust their driving modes or primitive driving patterns during normal driving [43].

Table III presents the statistical results of the durations of primitive driving patterns for all driving data using the three approaches. It can be found that HDP-HSMM obtains the amount of primitive driving patterns close to the sticky HDP-HMM, as highlighted in orange. In addition, the HDP-HSMM approach obtains the lowest percentage (0.0065) of primitive driving pattern whose duration is less than 1.0 s, compared to HDP-HMM with a percentage of 0.0216 and the sticky HDP-HMM with a percentage of 0.0441. It indicates that the HDP-HSMM method can segment time-series driving data into several satisfied segments and hold the primitive driving patterns. Therefore, in the following section, we will take driving style analysis and evaluation based on HDP-HSMM.

Fig. 10 presents the statistical results of pattern durations using the three approaches. It can be seen that most primitive driving patterns approximately fall in 3.93 s – 7.81 s range for HDP-HSMM and in 3.30 s – 7.64 s range for the sticky HDP-HMM. However, the HDP-HMM method obtains longer primitive pattern duration of 7.94 s on average, compared to the other two approaches. According to the segmentation results of the sticky HDP-HMM and HDP-HSMM, it can be concluded that human driver usually stays a specific driving mode with duration of 3.50 s – 10.0 s when following a lead vehicle. In addition, drivers sometimes could stay in specific but rare-occurred primitive driving patterns with duration longer than 20.0 s.

Fig. 11 shows the scattering results of primitive segments with all methods. It can be seen that HDP-HSMM (Fig. 11(c)) segments the time-series driving data into a set of reasonable primitive patterns with a lower switching frequency among driving modes, compared to other two approaches. For example, in the region A of Fig. 11, HDP-HMM fails to recognize the underlying patterns, and the sticky HDP-HMM characterizes the latent patterns with a high switching frequency and short pattern duration, which is not consistent with the case in real driving [43].

C. Labeling Behavioral Semantics

Based on the learned primitive driving patterns, the car-following behavior can be described by behavioral semantics defined as in Table II. In order to capture the dynamic process

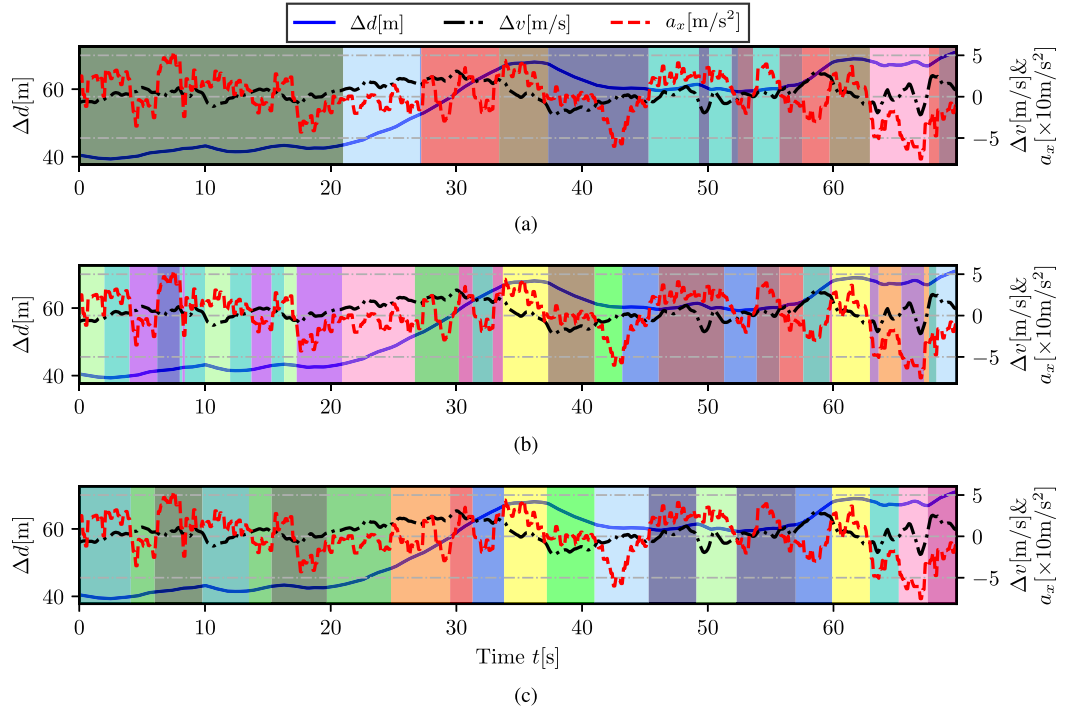


Fig. 9. Example of experiment results of one event for driver #0 using three different Bayesian nonparametric approaches. (a) HDP-HMM with 9 patterns. (b) sticky HDP-HMM with 17 patterns. (c) HDP-HSMM with 14 patterns.

TABLE III
STATISTICAL RESULTS OF DURATIONS OF PRIMITIVE DRIVING PATTERNS USING THREE METHODS FOR ALL DRIVING DATA

Methods	Total Number	Duration of primitive driving pattern (s)							
		< 1.0	[1.0, 5.0)	[5.0, 10.0)	[10.0, 15.0)	[15.0, 20.0)	[20.0, 25.0)	≥ 30.0	
HDP-HMM	18,174	0.0441	0.2819	0.4226	0.1534	0.0560	0.0228	0.0091	0.0102
sticky HDP-HMM	26,373	0.0216	0.5478	0.3276	0.0671	0.0213	0.0085	0.0032	0.0028
HDP-HSMM	24,591	0.0065	0.4713	0.4211	0.0714	0.0193	0.0056	0.0018	0.0030

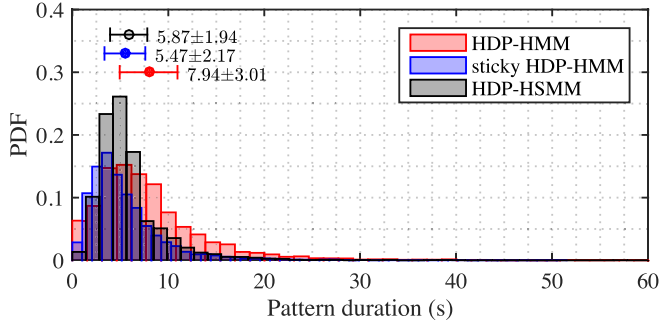


Fig. 10. Statistical results of primitive driving pattern durations.

of behavior, we describe each primitive driving pattern in car-following data sequences with the following interpretation:

“The driver is $S_{\Delta v}$ the lead vehicle by S_{a_x} in a $S_{\Delta d}$ ”

where

$$S_{\Delta v} \in \{RCI, CI, KE, FB, RFB\};$$

$$S_{a_x} \in \{AA, GA, NA, GD, AD\};$$

$$S_{\Delta d} \in \{LD, ND, CD\}.$$

For example, in the region B of bottom plot in Fig. 11, the relative range rate $\Delta v > 1.0$ m/s (i.e., $\{S_{\Delta v} = RFB\}$,

the range $\Delta d \in [47, 57]$ m (i.e., $S_{\Delta d} = ND$), and the absolute values of the acceleration mostly fall in $[0.05, 0.24]$ (i.e., $S_{a_x} = GA$ or $S_{a_x} = GD$). Thus, we can describe the driving behavior in region B as “The driver is rapidly falling behind the lead vehicle by gentle accelerating or decelerating in a normal distance.” Similarly, the driving behavior in region C can be described as “The driver is rapidly falling behind the lead vehicle by gentle accelerating in a long distance.” In the following section, to be simple, we represent drivers’ behavioral semantics by using a primitive pattern sequence such as $[S_{\Delta v}, S_{a_x}, S_{\Delta d}]$.

Based on the learned results, some primitive driving patterns are easy to be labeled with semantic elements, but some are not. In order to label driving patterns easily and find the commons in primitive driving patterns, we cluster the driving data of each segment into one single point to represent this primitive driving pattern. The K-means clustering method is applied in the light of its wide implementation to driving pattern classification [15], [47], [48]. The clustering results allow us to translate these primitive driving patterns in behavioral semantics. For instance, Fig. 12 presents the clustering result for driver #0 based on the segmentation results of HDP-HSMM. According to Table II, the pink point can be semantically interpreted as $[KE, AD, LD]$, that is, “The driver is keeping distance with

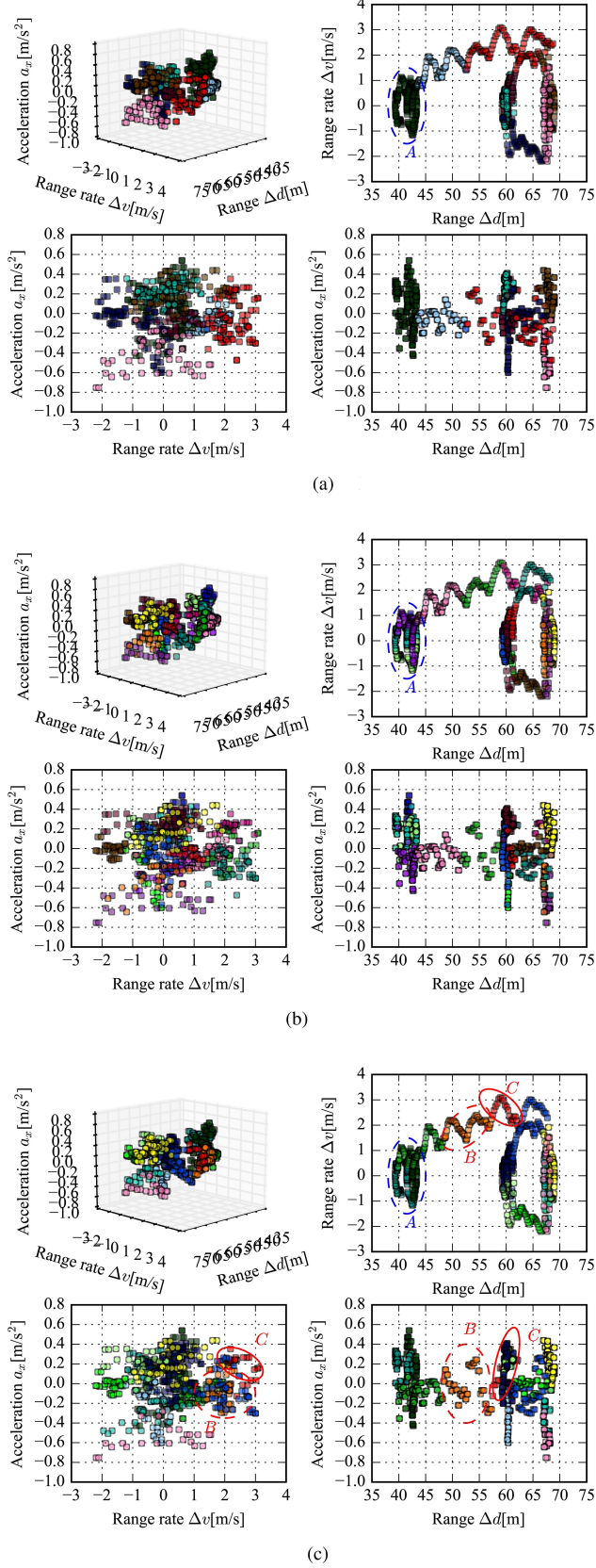


Fig. 11. Segment results with one event for driver #0 using three methods. (a) HDP-HMM. (b) sticky HDP-HMM. (c) HDP-HSMM.

the lead vehicle by *aggressive deceleration in a long distance.*”, corresponding to the pink points in the bottom plot of Fig. 11.

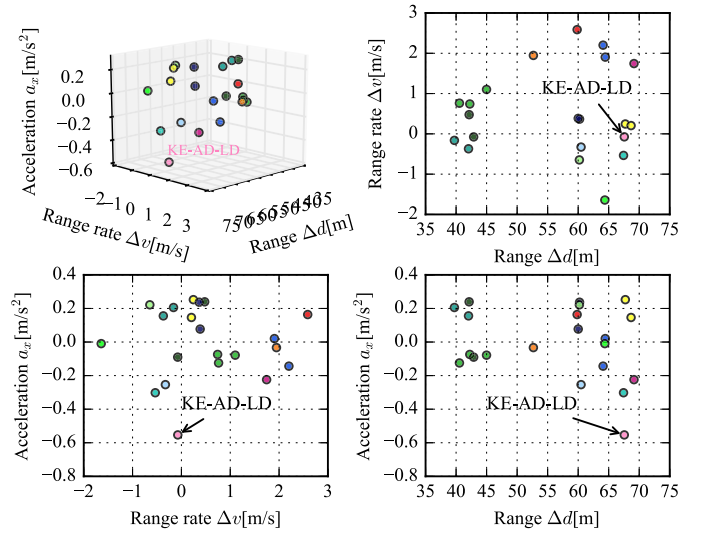


Fig. 12. Example of clustering results for driver #0 using K-means clustering based on HDP-HSMM with $K = 1$, where KE-AD-LD represents “keeping (KE) distance by aggressive deceleration (AD) in a long distance (LD)”.

V. DRIVING STYLE ANALYSIS BASED ON PRIMITIVE DRIVING PATTERNS

The above discussion indicates that the primitive driving patterns can provide a satisfied semantical way to analyze car-following behavior. In what follows, we will take driving style analysis based on the primitive driving patterns learned from HDP-HSMM.

A. Normalized Frequency Distribution of Driving Patterns

Instead of using the statistical metrics such as mean and standard deviation, we utilize the normalized frequency distribution of primitive driving patterns to characterize driving styles, which allows to take intuitive analysis. For each driver with L car-following events $Y_m = \{\mathbf{y}_m^{(l)}\}_{l=1}^L$, the normalized distribution of each pattern is computed by

$$f_{*,*}^{(m)} = \frac{N_{*,*}^{(m)}}{\sum_* N_{*,*}^{(m)}}, \quad * = [\mathbf{S}_{\Delta v}, \mathbf{S}_{\Delta d}] \quad (10)$$

where $N_{*,*}^{(m)}$ is the number of occurrences for driving pattern $*$ in Y_m based on the distance pattern $*$. Thus, we obtain the normalized frequency distribution for each driver with three distance patterns (i.e., close distance, normal distance, and long distance). Each primitive driving pattern is clustered and labeled according to Table II.

Fig. 13 shows examples of the normalized frequency distribution of primitive driving patterns for four drivers. Dark red represents that the driver has a high probability of acting in this pattern and dark blue represents that the driver has a low probability (nearly equal to zero) of driving in this pattern. For instance, when following a lead vehicle in a long distance (Fig. 13, bottom row), driver #0 (Fig. 13(a)) and driver #1 (Fig. 13(b)) prefer to rapidly close in the lead vehicle by no acceleration/deceleration, while driver #2 (Fig. 13(c)) and driver #3 (Fig. 13(d)) prefer falling behind by no acceleration/deceleration and gentle deceleration, respectively. When following the lead vehicle in a close or normal distance,

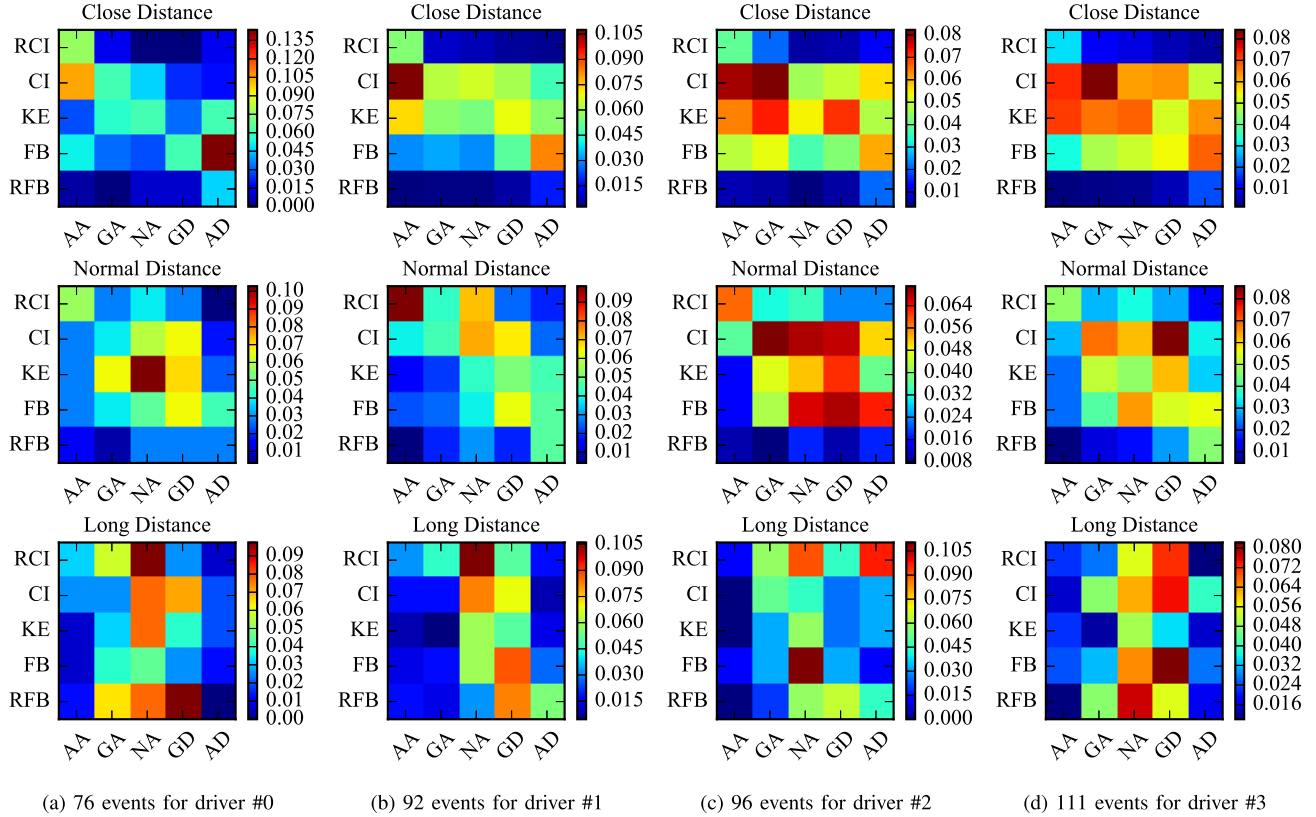


Fig. 13. Normalized frequency distributions of driving patterns for four drivers using HDP-HSMM. The dark red and dark blue indicate a higher and lower probability of driving in this pattern, respectively. RCI = rapidly closing in, CI = closing in, KE = keeping, FB = falling behind, RFB = rapidly falling behind, AA = aggressive acceleration, GA = gentle acceleration, NA = no acceleration, GD = gentle deceleration, AD = aggressive deceleration. (a) 76 events for driver #0. (b) 92 events for driver #1. (c) 96 events for driver #2. (d) 111 events for driver #3.

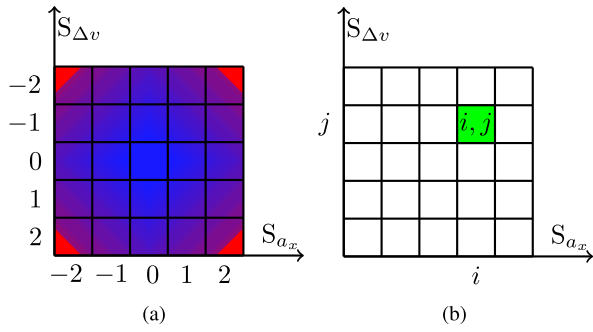


Fig. 14. The schematic diagram of (a) driving style patterns and (b) pattern index (i, j) for pattern $[S_{ax}, S_{\Delta v}]$.

our proposed approaches can also provide a semantic explanation for researchers.

In order to distinguish the driving pattern drivers prefer, we assign a unique index value to each primitive driving pattern (Fig. 14). The five levels of acceleration are labeled using integers from -2 to 2 , and the same operation for the range rate. A larger absolute value of the index indicates a more aggressive driving style, marked by dark red. Conversely, a smaller absolute value of the index represents a more gentle driving style, marked by dark blue, as shown in Fig. 14(a). The driving pattern with the highest normalized frequency probability in each distance pattern for the driver is treated as the most preferred one, represented using its index i and j (Fig. 14(b)). For instance, when following a lead vehicle with

TABLE IV
DRIVER'S PREFERENCE IN DRIVING PRIMITIVE
PATTERN (i, j) FOR ALL PARTICIPANTS

Driver No.	CD (i, j)	ND (i, j)	LD (i, j)
0	(2,1)	(0,0)	(1,2) or (0,-2)
1	(-2,-1)	(-2,-2)	(0,-2)
2	(-1,-1)	(-1,-1)	(0,1)
3	(-1,-1)	(1,-1)	(1,1)
4	(-2,-2)	(-2,-2)	(0,1)
5	(-2,-1)	(0,-1)	(0,-1)
6	(-2,-2)	(2,-1)	(1,-2)
7	(2,1)	(0,1)	(0,1)
8	(-2,0)	(1,1)	(0,1)
9	(2,1)	(1,-1)	(0,-1)
10	(-2,-1)	(1,0)	(0,-2)
11	(0,0)	(0,0)	(0,1)
12	(2,1)	(1,1)	(2,1)
13	(-2,-1)	(1,1)	(0,1)
14	(-2,-1)	(0,-1)	(0,-1)
15	(2,1)	(1,1)	(1,2)
16	(1,1)	(1,-1)	(0,1)
17	(-2,-2)	(-2,-2)	(1,-1)

CD = close distance; ND = normal distance; LD = long distance

a close distance, the primitive driving pattern that driver #0 prefers is [FB, AD], denoted as the dark red in the top plot of Fig. 13(a). Table IV lists the index value (i, j) of the most preferred primitive driving patterns for every driver, where i and j represent the levels of acceleration/deceleration and range rate, respectively. According to Table IV, it can be concluded:

- When following a lead vehicle in a close distance, most drivers prefer falling behind or closing in

(i.e., $j = -1$ or 1) the lead vehicle by taking an aggressive acceleration or deceleration (i.e., $i = -2$ or 2), except for driver #11 (blue shade) who prefers to keep a constant headway by no acceleration/deceleration. In addition, driver #4, driver #6, and driver #17 (red shade) prefer to rapidly fall behind (i.e., $j = -2$) the lead vehicle by accelerating aggressively (i.e., $i = -2$).

- When following a lead vehicle in a normal distance, most drivers prefer falling behind or closing in (i.e., $j = 1$ or 1) the lead vehicle by taking a gentle deceleration (i.e., $i = 1$), except for driver #1, driver #4, and driver #17 (orange shade) who prefer rapidly closing in the lead vehicle (i.e., $j = -2$) by accelerating aggressively (i.e., $i = -2$).
- When following a lead vehicle in a long distance, most drivers prefer closing in (i.e., $j = 1$) with no acceleration/deceleration (i.e., $i = 0$), except for driver #0, driver #2, driver #6, driver #12, and driver #15 shaded by light gray. For example, driver #12 prefers falling behind by taking an aggressive deceleration.

The above analysis demonstrates that our proposed framework based on primitive driving patterns provides a semantic way to analyze driving style, compared to only using the statistical metrics such as mean and standard deviation.

B. Interdriver Differences in Driving Style

According to the above discussion, the normalized distribution of primitive driving patterns is able to describe and analyze individual driving styles. In this section, we will present the similarity measure of driving styles between drivers. Differing previous research using statistical metrics of driving data to capture driver's driving style, we select the normalized distribution of primitive driving patterns as the indicators. It is common to assume a normal distribution for the indicators and to compare their mean and standard deviation [38] when comparing the driving styles of two drivers. Here, we are not restricted by the limitations of this assumption and we compute the similarity of two drivers in driving styles using the Kullback-Leibler (KL) divergence [33], [40] between two corresponding distributions to measure the similarity between drivers. The KL divergence of the normalized distribution of primitive driving patterns between drivers m_i and m_j is defined as

$$D_{KL}^{(*)}(F^{(m_i)} \parallel F^{(m_j)}) = - \sum_{\star} f_{\star,*}^{(m_i)} \log \left(\frac{f_{\star,*}^{(m_i)}}{f_{\star,*}^{(m_j)}} \right) \quad (11)$$

where \star and $*$ are defined same as in (10). A large value of KL divergence indicates a big difference between two drivers. For example, when $m_i = m_j$, it implies that the driver is compared to him/herself, thus we have $D_{KL}^{(*)}(F^{(m_i)} \parallel F^{(m_j)}) = 0$.

Fig. 15 presents the KL divergence of each pairs of drivers. Dark red represents the great difference between two drivers and dark blue represents that drivers are similar to each other regarding driving styles. Fig. 15(a) indicates that when closely following a lead vehicle, driver behavior of driver #8 is different from driver #12, marked with the dark red. According to Fig. 15(b), when following the lead vehicle at a

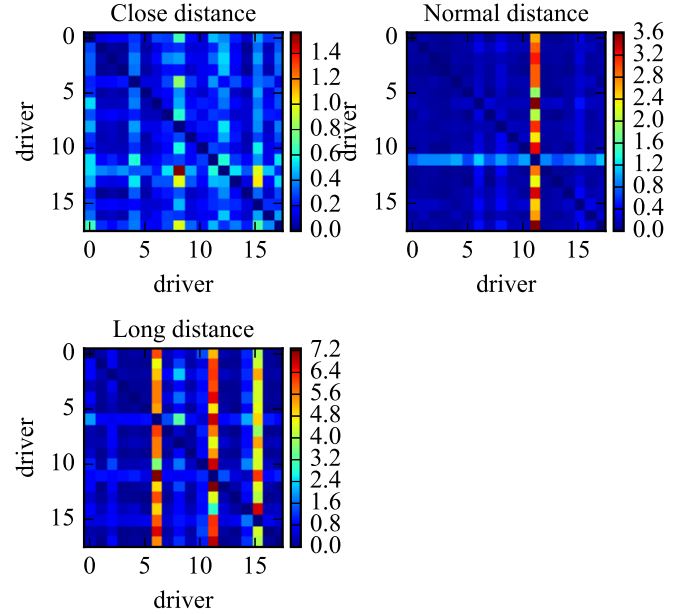


Fig. 15. KL divergence between two normalized distributions of primitive driving patterns among all drivers.

normal distance, driver #11 is much different from others as there exists a red vertical bar between driver #11 and all other drivers. When following a long distance to the lead vehicle (Fig. 15(c)), driver #6, driver #11, and driver #15 behave much differently from others. Therefore, the KL divergence index combining with primitive driving patterns enables to visualize the similarity in driving styles between drivers from a semantical perspective.

VI. CONCLUSION AND DISCUSSION

This paper proposed a novel framework for driving style analysis by using primitive driving patterns with the Bayesian nonparametric approaches. A set of primitive driving patterns were learned from time-series driving data with priorly unknown these patterns. To achieve this, a hierarchical structure (i.e., HDP-HSMM) was developed by combining a hierarchical Dirichlet process (HDP) and a hidden semi-Markov model (HSMM). Comprehensive comparison between HDP-HSMM and other Bayesian nonparametric methods (HDP-HMM and sticky HDP-HMM) was made for driver's car-following behavior analysis. And we found that HDP-HSMM can learn a set of satisfied primitive driving patterns. These learned primitive driving patterns were used to define car-following behavioral semantics according to drivers' physical and psychological perception thresholds. Their normalized frequency distribution was then applied for individual driving style analysis. Experimental results demonstrated that the utilization of primitive driving pattern provides a semantic and visualizable way for driving style analysis.

Our future work will be articulated around two axes. The first one is to utilize the primitive driving patterns to learn a classifier able to semantically recognize driving styles, instead of using the static statistical metrics of measured variables. In this way, the driving style could be potentially detected and semantically explained. The primitive driving patterns could also be learned by using nonlinear Bayesian estimation [49].

Our second objective is to apply the learned classifier to improve vehicle performance for individual drivers. Semantic analysis of driver behavior could help gain insights into the underlying relations between driving style and specific vehicle performance. For example, in order to make eco-driving control systems personalizable for a driver, we could analyze the influence of driving style on fuel consumption [50] with behavioral semantics and find a personalized control strategy adaptable to this person's behavior.

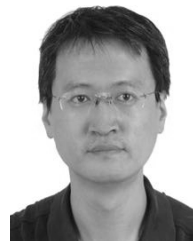
REFERENCES

- [1] S. Di Cairano, D. Bernardini, A. Bemporad, and I. V. Kolmanovsky, "Stochastic MPC with learning for driver-predictive vehicle control and its application to HEV energy management," *IEEE Trans. Control Syst. Technol.*, vol. 22, no. 3, pp. 1018–1031, May 2014.
- [2] F. Sagberg, Selpi, G. F. B. Piccinini, and J. Engström, "A review of research on driving styles and road safety," *Human Factors*, vol. 57, no. 7, pp. 1248–1275, 2015.
- [3] C. M. Martinez, M. Heucke, F.-Y. Wang, B. Gao, and D. Cao, "Driving style recognition for intelligent vehicle control and advanced driver assistance: A survey," *IEEE Trans. Intell. Transp. Syst.*, vol. 19, no. 3, pp. 666–676, Mar. 2018.
- [4] W. Wang, J. Xi, C. Liu, and X. Li, "Human-centered feed-forward control of a vehicle steering system based on a driver's path-following characteristics," *IEEE Trans. Intell. Transp. Syst.*, vol. 18, no. 6, pp. 1440–1453, Jun. 2016.
- [5] M. Rafael, M. Sanchez, V. Mucino, J. Cervantes, and A. Lozano, "Impact of driving styles on exhaust emissions and fuel economy from a heavy-duty truck: Laboratory tests," *Int. J. Heavy Vehicle Syst.*, vol. 13, nos. 1–2, pp. 56–73, 2006.
- [6] Y. L. Murphrey, R. Milton, and L. Kiliaris, "Driver's style classification using jerk analysis," in *Proc. IEEE Workshop Comput. Intell. Vehicles Veh. Syst. (CIVVS)*. Nashville, TN, USA, Mar./Apr. 2009, pp. 23–28.
- [7] L. Xu, J. Hu, H. Jiang, and W. Meng, "Establishing style-oriented driver models by imitating human driving behaviors," *IEEE Trans. Intell. Transp. Syst.*, vol. 16, no. 5, pp. 2522–2530, Oct. 2015.
- [8] B. Shi *et al.*, "Evaluating driving styles by normalizing driving behavior based on personalized driver modeling," *IEEE Trans. Syst., Man, Cybern., Syst.*, vol. 45, no. 12, pp. 1502–1508, Dec. 2015.
- [9] J. Felipe, J. C. Amarillo, J. E. Naranjo, F. Serradilla, and A. Díaz, "Energy consumption estimation in electric vehicles considering driving style," in *Proc. IEEE 18th Int. Conf. Intell. Transp. Syst. (ITSC)*, Sep. 2015, pp. 101–106.
- [10] V. Vaikus, P. Lengvenis, and G. Žylius, "Driving style classification using long-term accelerometer information," in *Proc. 19th Int. Conf. Methods Models Automat. Robot. (MMAR)*, Miedzyzdroje, Poland, Sep. 2014, pp. 641–644.
- [11] O. Taubman-Ben-Ari and V. Skvirsky, "The multidimensional driving style inventory a decade later: Review of the literature and re-evaluation of the scale," *Accident Anal. Prevention*, vol. 93, pp. 179–188, Aug. 2016.
- [12] M. Van Ly, S. Martin, and M. M. Trivedi, "Driver classification and driving style recognition using inertial sensors," in *Proc. IEEE Intell. Vehicles Symp. (IV)*, Gold Coast, QLD, Australia, Jun. 2013, pp. 1040–1045.
- [13] G. S. Aoude, V. R. Desaraju, L. H. Stephens, and J. P. How, "Driver behavior classification at intersections and validation on large naturalistic data set," *IEEE Trans. Intell. Transp. Syst.*, vol. 13, no. 2, pp. 724–736, Jun. 2012.
- [14] W. Wang, J. Xi, A. Chong, and L. Li, "Driving style classification using a semisupervised support vector machine," *IEEE Trans. Human-Mach. Syst.*, vol. 47, no. 5, pp. 650–660, Oct. 2017.
- [15] B. Higgs and M. Abbas, "Segmentation and clustering of car-following behavior: Recognition of driving patterns," *IEEE Trans. Intell. Transp. Syst.*, vol. 16, no. 1, pp. 81–90, Feb. 2015.
- [16] H. Okuda, N. Ikami, T. Suzuki, Y. Tazaki, and K. Takeda, "Modeling and analysis of driving behavior based on a probability-weighted ARX model," *IEEE Trans. Intell. Transp. Syst.*, vol. 14, no. 1, pp. 98–112, Mar. 2013.
- [17] S. Sekizawa *et al.*, "Modeling and recognition of driving behavior based on stochastic switched ARX model," *IEEE Trans. Intell. Transp. Syst.*, vol. 8, no. 4, pp. 593–606, Dec. 2007.
- [18] D. A. Johnson and M. M. Trivedi, "Driving style recognition using a smartphone as a sensor platform," in *Proc. 14th Int. IEEE Conf. Intell. Transp. Syst. (ITSC)*, Washington, DC, USA, Oct. 2011, pp. 1609–1615.
- [19] C. MacAdam, Z. Bareket, P. Fancher, and R. Ervin, "Using neural networks to identify driving style and headway control behavior of drivers," *Vehicle Syst. Dyn.*, vol. 29, no. S1, pp. 143–160, 1998.
- [20] Q. H. Do, H. Tehrani, S. Mita, M. Egawa, K. Muto, and K. Yoneda, "Human drivers based active-passive model for automated lane change," *IEEE Intell. Transp. Syst. Mag.*, vol. 9, no. 1, pp. 42–56, Jan. 2017.
- [21] J. Nilsson, J. Silvlin, M. Brännström, E. Coelingh, and J. Fredriksson, "If, when, and how to perform lane change maneuvers on highways," *IEEE Intell. Transp. Syst. Mag.*, vol. 8, no. 4, pp. 68–78, Oct. 2016.
- [22] J. Nilsson, M. Brännström, E. Coelingh, and J. Fredriksson, "Lane change maneuvers for automated vehicles," *IEEE Trans. Intell. Transp. Syst.*, vol. 18, no. 5, pp. 1087–1096, May 2016.
- [23] J. Taylor, X. Zhou, N. M. Routhail, and R. J. Porter, "Method for investigating intradriver heterogeneity using vehicle trajectory data: A dynamic time warping approach," *Transp. Res. B, Methodol.*, vol. 73, pp. 59–80, Mar. 2015.
- [24] X. Ma and I. Andreasson, "Behavior measurement, analysis, and regime classification in car following," *IEEE Trans. Intell. Transp. Syst.*, vol. 8, no. 1, pp. 144–156, Mar. 2007.
- [25] R. Hamada *et al.*, "Modeling and prediction of driving behaviors using a nonparametric Bayesian method with AR models," *IEEE Trans. Intell. Veh.*, vol. 1, no. 2, pp. 131–138, Jun. 2016.
- [26] T. Taniguchi, S. Nagasaka, K. Hitomi, N. P. Chandrasiri, T. Bando, and K. Takenaka, "Sequence prediction of driving behavior using double articulation analyzer," *IEEE Trans. Syst., Man, Cybern., Syst.*, vol. 46, no. 9, pp. 1300–1313, Sep. 2016.
- [27] T. Taniguchi, S. Nagasaka, K. Hitomi, K. Takenaka, and T. Bando, "Unsupervised hierarchical modeling of driving behavior and prediction of contextual changing points," *IEEE Trans. Intell. Transp. Syst.*, vol. 16, no. 4, pp. 1746–1760, Aug. 2015.
- [28] S.-Z. Yu, "Hidden semi-Markov models," *Artif. Intell.*, vol. 174, no. 2, pp. 215–243, Feb. 2010.
- [29] L. Rabiner, "A tutorial on hidden Markov models and selected applications in speech recognition," *Proc. IEEE*, vol. 77, no. 2, pp. 257–286, Feb. 1989.
- [30] M. J. Johnson and A. S. Willsky, "Bayesian nonparametric hidden semi-Markov models," *J. Mach. Learn. Res.*, vol. 14, no. 1, pp. 673–701, 2013.
- [31] Y. W. Teh, M. I. Jordan, M. J. Beal, and D. M. Blei, "Hierarchical Dirichlet processes," *J. Amer. Statist. Assoc.*, vol. 101, no. 476, pp. 1566–1581, Dec. 2006.
- [32] E. Fox, E. B. Sudderth, M. I. Jordan, and A. S. Willsky, "Bayesian nonparametric inference of switching dynamic linear models," *IEEE Trans. Signal Process.*, vol. 59, no. 4, pp. 1569–1585, Apr. 2011.
- [33] Z. Mahboubi and M. J. Kochenderfer, "Learning traffic patterns at small airports from flight tracks," *IEEE Trans. Intell. Transp. Syst.*, vol. 18, no. 4, pp. 917–926, Apr. 2017.
- [34] T. Rydén, "EM versus Markov chain Monte Carlo for estimation of hidden Markov models: A computational perspective," *Bayesian Anal.*, vol. 3, no. 4, pp. 659–688, 2008.
- [35] D. F. Wulsin, E. B. Fox, and B. Litt, "Modeling the complex dynamics and changing correlations of epileptic events," *Artif. Intell.*, vol. 216, pp. 55–75, Nov. 2014.
- [36] W. Wang, D. Zhao, J. Xi, and W. Han, "A learning-based approach for lane departure warning systems with a personalized driver model," *IEEE Trans. Veh. Technol.*, vol. 67, no. 10, pp. 9145–9157, Oct. 2018, doi: [10.1109/TVT.2018.2854406](https://doi.org/10.1109/TVT.2018.2854406).
- [37] W. Wang, D. Zhao, J. Xi, D. J. LeBlanc, and J. K. Hedrick, "Development and evaluation of two learning-based personalized driver models for car-following behaviors," in *Proc. Amer. Control Conf.*, Seattle, WA, USA, May 2017, pp. 1133–1138.
- [38] S. Lefèvre, A. Carvalho, and F. Borrelli, "A learning-based framework for velocity control in autonomous driving," *IEEE Trans. Autom. Sci. Eng.*, vol. 13, no. 1, pp. 32–42, Jan. 2016.
- [39] M. Brackstone and M. McDonald, "Car-following: A historical review," *Transp. Res. F, Traffic Psychol. Behavior*, vol. 2, no. 4, pp. 181–196, 1999.
- [40] W. Wang, C. Liu, and D. Zhao, "How much data are enough? A statistical approach with case study on longitudinal driving behavior," *IEEE Trans. Intell. Veh.*, vol. 2, no. 2, pp. 85–98, Jun. 2017.
- [41] C. M. Bishop, *Pattern Recognition and Machine Learning*. New York, NY, USA: Springer, 2007.
- [42] K. I. Ahmed, "Modeling drivers' acceleration and lane changing behavior," Ph.D. dissertation, Dept. Civil Environ. Eng., Massachusetts Inst. Technol., Cambridge, MA, USA, 1999.

- [43] H.-H. Yang and H. Peng, "Development of an errorable car-following driver model," *Vehicle Syst. Dyn.*, vol. 48, no. 6, pp. 751–773, 2010.
- [44] M. Fischer, L. Eriksson, and K. Oeltze, "Evaluation of methods for measuring speed perception in a driving simulator," in *Proc. Driving Simulation Conf. Eur.*, S. Espié, A. Kemeny, and F. Mérienne, Eds. Paris, France: 2012, pp. 214–229.
- [45] C. C. Macadam, "Understanding and modeling the human driver," *Swets Zeitlinger, Vehicle Syst. Dyn.*, vol. 40, nos. 1–3, pp. 101–134, 2003.
- [46] P. Ioannou *et al.*, "Precursor systems analysis for automated highway systems: Lateral, and longitudinal control," Center Adv. Transp. Technol., Federal Highway Admin., Univ. Southern California, Los Angeles, CA, USA, Tech. Rep. FHWA-RD-95-095, 1994, vol. 2.
- [47] W. Wang and J. Xi, "A rapid pattern-recognition method for driving styles using clustering-based support vector machines," in *Proc. Amer. Control Conf. (ACC)*, Boston, MA, USA, Jul. 2016, pp. 5270–5275.
- [48] S. Wang, Y. Zhang, C. Wu, F. Darvas, and W. A. Chaovalltwongse, "Online prediction of driver distraction based on brain activity patterns," *IEEE Trans. Intell. Transp. Syst.*, vol. 16, no. 1, pp. 136–150, Feb. 2015.
- [49] H. Fang, N. Tian, Y. Wang, M. Zhou, and M. A. Haile, "Nonlinear Bayesian estimation: from kalman filtering to a broader horizon," *IEEE/CAA J. Autom. Sinica*, vol. 5, no. 2, pp. 401–417, Mar. 2018.
- [50] M. Zhou, H. Jin, and W. Wang, "A review of vehicle fuel consumption models to evaluate eco-driving and eco-routing," *Transp. Res. D, Transp. Environ.*, vol. 49, pp. 203–218, Dec. 2016.



Wenshuo Wang (S'15) received the B.S. degree in transportation engineering from the Shandong University of Technology, Shandong, China, in 2012. He is currently pursuing the Ph.D. degree in mechanical engineering with the Beijing Institute of Technology. From 2015 to 2017, he was studying at the Department of Mechanical Engineering, University of California at Berkeley (UCB). He is now studying at the Department of Mechanical Engineering, University of Michigan, Ann Arbor. His work focuses on modeling and recognizing driver's behavior, making intelligent control systems between human driver and vehicle.



Junqiang Xi received the B.S. degree in automotive engineering from the Harbin Institute of Technology, Harbin, China, in 1995, and the Ph.D. degree in vehicle engineering from the Beijing Institute of Technology (BIT), Beijing, China, in 2001. In 2001, he joined the State Key Laboratory of Vehicle Transmission, BIT. From 2012 to 2013, he conducted research as an Advanced Research Scholar at the Vehicle Dynamic and Control Laboratory, The Ohio State University, OH, USA. He is currently a Professor and the Director of the Automotive Research Center, BIT. His research interests include vehicle dynamic and control, power-train control, mechanics, intelligent transportation systems, and intelligent vehicles.



Ding Zhao received the Ph.D. degree from the University of Michigan, Ann Arbor, MI, USA, in 2016. He is currently an Assistant Research Scientist in mechanical engineering with the University of Michigan. His research interests include autonomous vehicles, intelligent transportation, connected vehicles, dynamics and control, human-machine interaction, machine learning, and big data analysis.